Research Paper

Assessing the Impact of Urban Residential Morphology on the Seasonal Variation of Building Energy Consumption in Severely Cold Regions

Evidence from Harbin, China

Junyang ZHAO, School of Architecture and Design, Harbin Institute of Technology; Key Laboratory of National Territory Spatial Planning and Ecological Restoration in Cold Regions, Ministry of Natural Resources, China

Lulu CHEN (Correspondence), School of Architecture and Design, Harbin Institute of Technology; Key Laboratory of National Territory Spatial Planning and Ecological Restoration in Cold Regions, Ministry of Natural Resources, China; chenlulu@hit.edu.cn, Tel: +86 137 6689 6981

Haoting TANG, School of Architecture and Design, Harbin Institute of Technology; Key Laboratory of National Territory Spatial Planning and Ecological Restoration in Cold Regions, Ministry of Natural Resources, China

Abstract

Urban residential areas are major contributors to building energy consumption and are strongly shaped by their spatial morphological characteristics. In severely cold regions, extreme heating demands in winter and cooling needs in summer produce pronounced seasonal differences in residential energy use. Understanding how urban residential morphology drives these seasonal variations is essential for low-carbon urban planning and climate-resilient neighborhood design.

This study focuses on Harbin, China, and investigates 15 sampled residential areas across three seasonal periods — winter (November–December), summer (July–August), and transitional season (September–October) — defined by regional climatic patterns. A multi-source spatial morphology database of 26 indicators was developed. Honeybee and EnergyPlus were used to simulate neighborhood-scale energy use intensity (EUI) for each season. Spearman's correlation analysis identified Spatial Morphology Key Factors (SMKFs) per season, which were then entered into three multiple linear regression models.

Results show that: (1) FAR, building layout pattern, and building density are significantly correlated with residential energy use across all seasons; (2) EUI varies markedly among the three periods, confirming the seasonal nature of energy demand; and (3) distinct sets of spatial morphology factors drive energy use in each season. These findings provide an evidence base for seasonally differentiated, morphology-sensitive planning strategies that support climate resilience in severely cold urban regions.

Keywords

severely cold regions, urban residential areas, spatial morphology, building energy consumption, influencing factors, seasonal variation

1. Introduction

Buildings consume approximately 30% of the world's total energy, with heating alone accounting for nearly half of that share (Staffell, I. et al. 2023). In severely cold regions, long heating seasons, increasingly extreme weather events, and rising thermal comfort standards mean that residential energy demand remains high across much of the year (Hao, Z. et al. 2022). In Harbin, northeast China, the official heating season spans approximately 180 days, placing urgent pressure on planners and engineers to reduce seasonal energy loads (Liu, Y.L. et al. 2018; Wang, D. et al. 2025). Identifying morphology-based planning strategies that minimise these loads is therefore a critical step toward reconciling climate adaptation with energy security (Wang, M. et al. 2025).

The three-dimensional arrangement of buildings and open spaces — collectively described as urban morphology — significantly affects a neighbourhood's heating and cooling demands. Building density and height govern solar access and shading patterns, while urban canyon geometry and green space availability alter local microclimates such as temperature and wind flow (Sun, C. et al. 2022; Khalvandi, R. et al. 2023; Han, D. et al. 2025). Energy efficiency at the neighbourhood scale is thus shaped not only by individual building design but also by the collective spatial configuration of each residential area (Li, H. et al. 2025; Quan, S.J. et al. 2025).

Despite growing interest in this field, important gaps remain. Most existing studies use annual energy totals or peak winter demand as their primary indicators, which obscures how morphology influences energy use differently across climatic seasons (Lin, Z. et al. 2024; Wang, M. et al. 2025). For severely cold climates, this is a significant shortcoming: planners must simultaneously manage heavy winter heating loads, transitional-season envelope heat transfer, and increasing summer cooling demands driven by climate change (Xu, X. et al. 2024). Furthermore, empirical work has focused predominantly on individual buildings or commercial districts, leaving residential neighbourhoods as collective spatial units relatively understudied (Rahimi Gharibvand, F. et al. 2025). Methodologically, hybrid approaches combining simulation with statistical analysis have rarely been applied to examine granular, season-specific morphology–energy relationships (Adilkhanova, I. et al. 2023). These gaps limit the development of climate-responsive, seasonally differentiated planning guidelines for cold-region cities.

This study contributes: (1) a season-disaggregated energy database for a severely cold-region city; (2) empirical identification of SMKFs for each season; and (3) evidence-based morphological guidelines applicable to climate-resilient neighbourhood planning and urban renewal.

2. Methodology

This study employs a mixed simulation–statistical approach. Simulated energy consumption data are generated for residential neighbourhoods using building energy models, and statistical analysis is then applied to identify relationships between morphological variables and seasonal energy use intensity.

2.1. Study Subject

Fifteen residential neighbourhoods in Harbin were selected to capture a wide range of morphological types, including perimeter-block, slab-row, and point-tower configurations (Xu, X. et al. 2024; Shen, P. et al. 2024). Neighbourhoods span construction periods from 1965 to 2020, representing the dominant residential typologies of the city (Aldawoud, A. et al. 2008; Anon 2018; Pan, W. et al. 2022).

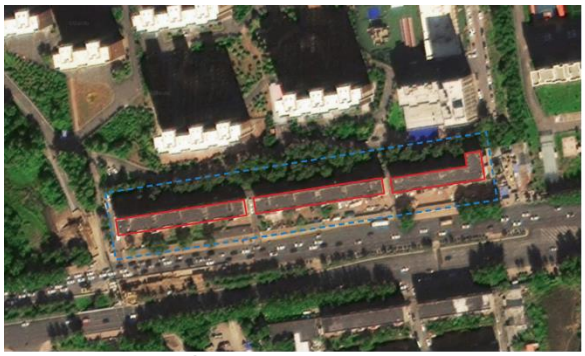

Satellite view of residential area NO.4, the Linear Block Residential Area



Satellite view of residential area NO.5, the Point Block Residential Area



Satellite view of residential area NO.7, the Slab Block Residential Area



Satellite view of residential area NO.10, the Perimeter Block Residential Area

Figure 1. Satellite view of residential areas selected

A 26-indicator spatial morphology database was developed through literature review, web-based data collection (OpenStreetMap, Starmap Cloud, Google Satellite), and field surveys. Indicators were organised into three categories — development intensity, facade interface, and spatial configuration — and screened to eliminate collinear or redundant variables (Quan, S.J. et al. 2021; Wang, Y. et al. 2024a; Guillén-Mena, V. et al. 2024; Liu, G. et al. 2025). Key indicators are listed in Table 1.

Table 1. Key spatial and morphological parameters.

Morphology Category	Indicator Name	Definition	Calculation Formula	Data source
Development Intensity	Floor Area Ratio (FAR)	Ratio of total building floor area to the site area	FAR = Total Building Floor Area / Site Area	OpenStreetMap; China's Third National Land Survey (2020)
	Building Density (BD)	Ratio of total building footprint area to the site area	BD = Total Building Footprint / Site Area	OpenStreetMap; Google Satellite Imag
Spatial configuration	Building Layout Pattern (BLP)	Spatial arrangement type of buildings (e.g., row, tower, mixed)	BLP = Categorical classification based on spatial configuration	Google Satellite Images; Field survey
	Average Building Height (ABH)	Weighted average height of all buildings in the sample block	ABH = Σ(Building Floor Area × Height) / Total Floor Area	Starmap Cloud; Field survey
	Number of High-rise Buildings (NHB)	Count of buildings exceeding 24 meters (8 stories) in height	NHB = Count(hi > 24m)	Starmap Cloud; OpenStreetMap

	Maximum Building Height (BHmax)	Height of the tallest building within the sample block	BHmax = max{h_1, h_2, ..., hn}	Starmap Cloud; Field survey
	Ratio of High-rise Buildings (RHB)	Proportion of high-rise buildings to total building count	RHB = Number of High-rise Buildings / Total Buildings	OpenStreetMap; Google Satellite Images
	Height Standard Deviation (HSD)	Measure of height variation among buildings in the block	HSD = √[Σ(hi - ABH)² / n]	Starmap Cloud; OpenStreetMap
	Average Building Footprint Area (ABFA)	Mean footprint area of all buildings within the sample block	ABFA = Σ(Building Footprint) / Number of Buildings	OpenStreetMap; Google Satellite Images
	Average Building Volume (ABV)	Mean volume of all buildings within the sample block	ABV = Σ(Footprint × Height) / Number of Buildings	Starmap Cloud; OpenStreetMap
	Window-to-Wall Ratio (WWR)	Ratio of window area to total exterior wall area	WWR = Total Window Area / Total Wall Area	Field survey
	Sky View Factor (SVF)	Ratio of visible sky hemisphere from ground level to total hemisphere	SVF = Visible Sky Solid Angle / 2π steradians Range: 0 (completely obstructed) to 1 (fully open)	Google Satellite Images; Field survey
Facade interface	Facade Unevenness (FU)	Degree of protrusions and recessions on building facades	FU = Standard Deviation of Facade Depth Variations	Field survey
	Facade Roughness (FR)	Measure of surface irregularity of building facades	FR = Actual Facade Surface Area / Projected Facade Area	Field survey
	Facade Opening Characteristics (FOC)	Distribution pattern and size of openings (windows, doors) on facades	FOC = f(Opening Size, Distribution, Frequency)	Field survey

Note: Data sources: OpenStreetMap (http://www.openstreetmap.org); Starmap Cloud (https://www.starmapcloud.com); Google Satellite Images (https://www.maps.google.com); China's Third National Land Survey 2020 (https://www.mnr.gov.cn); Field surveys conducted by the authors.

2.2. Framework of method

The research follows four sequential steps (Figure 2):

Step 1: Establish a 26-indicator spatial morphology database for 15 residential neighbourhoods through literature review, web-based data collection, and field surveys.

Step 2: Simulate seasonal energy use intensity (EUI, kWh/m²) for each neighbourhood using the Honeybee–EnergyPlus model within Grasshopper, covering three seasonal periods — winter (November–December), summer (July–August), and transitional season (September–October).

Step 3: Apply Spearman's correlation analysis and multiple linear regression to identify SMKFs per season and quantify morphology–energy relationships.

Step 4: Synthesise findings into evidence-based morphological guidelines for energy-efficient, climate-resilient residential planning in severely cold regions.

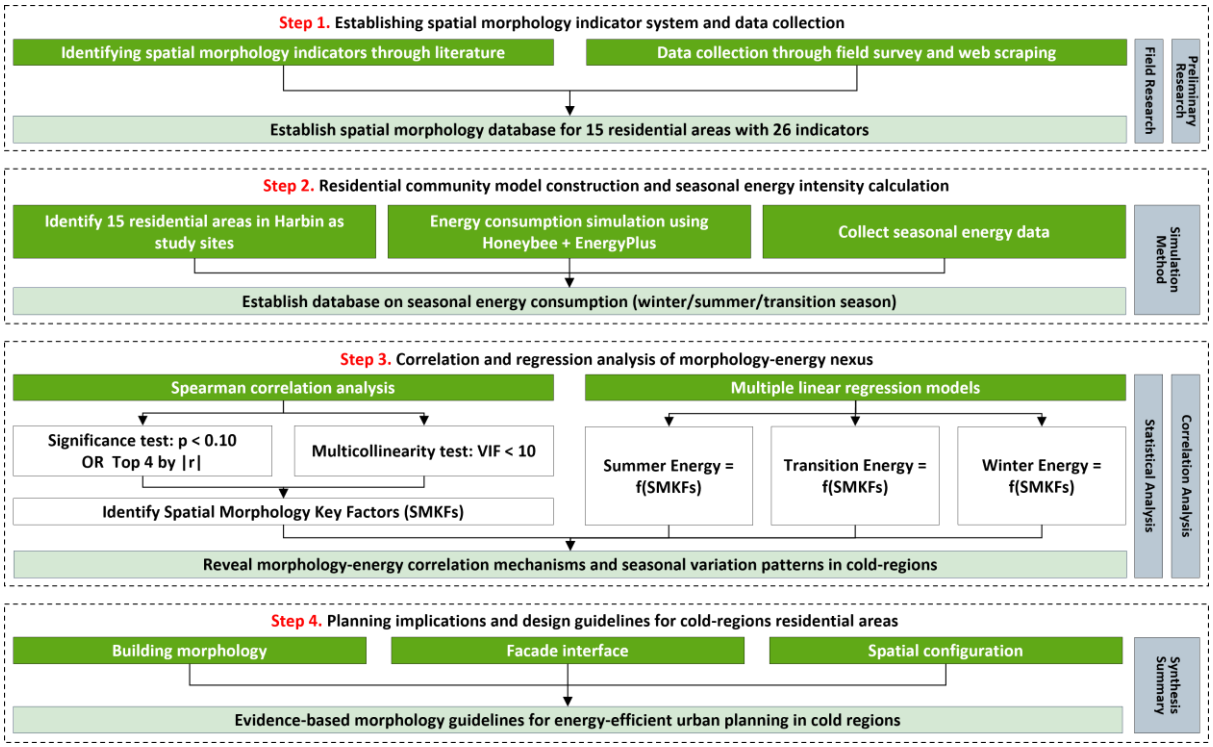

Figure 2. Research framework.

2.2.1. Energy simulation

Neighbourhood energy models were constructed using the Honeybee–EnergyPlus plug-in within Grasshopper (Ferrando et al., 2020). Three-dimensional neighbourhood geometries were generated from multi-source spatial data. Building envelope parameters were set in accordance with the General Code for Energy Conservation and Renewable Energy Utilization in Buildings (GB 55015-2021) and Design Standards for Energy Efficient Residential Buildings in Severely Cold and Cold Zones (JGJ 26-2018). Weather inputs used the Hourly Typical Meteorological Year dataset for Harbin (HAR).

Simulations were run separately for three seasonal operation scenarios. The winter scenario modelled space heating loads only (cooling off). The summer scenario modelled cooling loads only (heating off). The transitional-season scenario modelled natural ventilation, envelope heat transfer, and internal gains, with bounded heating and cooling thresholds (Balali, Y. et al. 2023; Wang, Z. et al. 2024). Holding non-morphological parameters constant across all neighbourhoods enabled direct attribution of EUI differences to spatial morphology (Jalilian, R. et al. 2025).

2.2.2. Correlation and regression

Spearman's rank correlation coefficients were calculated between the 26 morphological indicators and seasonal EUI values. Indicators were retained as SMKFs if they met a significance threshold of $p < 0.10$ or ranked in the Top 4 by $|r|$. Collinear variables (VIF ≥ 10) were excluded (Menberg, K. et al. 2016; Song, S. et al. 2020). This process yielded three season-specific SMKF sets, each used to build a separate multiple linear regression model. Model performance was evaluated using adjusted R^2, F-statistics, residual normality tests, and heteroscedasticity diagnostics. Regression coefficients were standardised (β) to allow cross-season comparisons of indicator importance.

3. Discussion

3.1. Seasonal patterns of neighbourhood energy intensity

Simulated EUI across the 15 Harbin neighbourhoods confirms a strongly seasonal pattern. Mean winter EUI is 161.3 kWh/m² — approximately 4.5 times the summer mean (36.1 kWh/m²) and 2.7 times the transitional season mean (59.3 kWh/m²). Proportional shares across the year are: winter 63%, transitional season 23%, and summer 14% (Figure 3). Winter dominates, but the remaining 37% of seasonal demand underscores the need for a full-season morphological assessment rather than a heating-only approach.

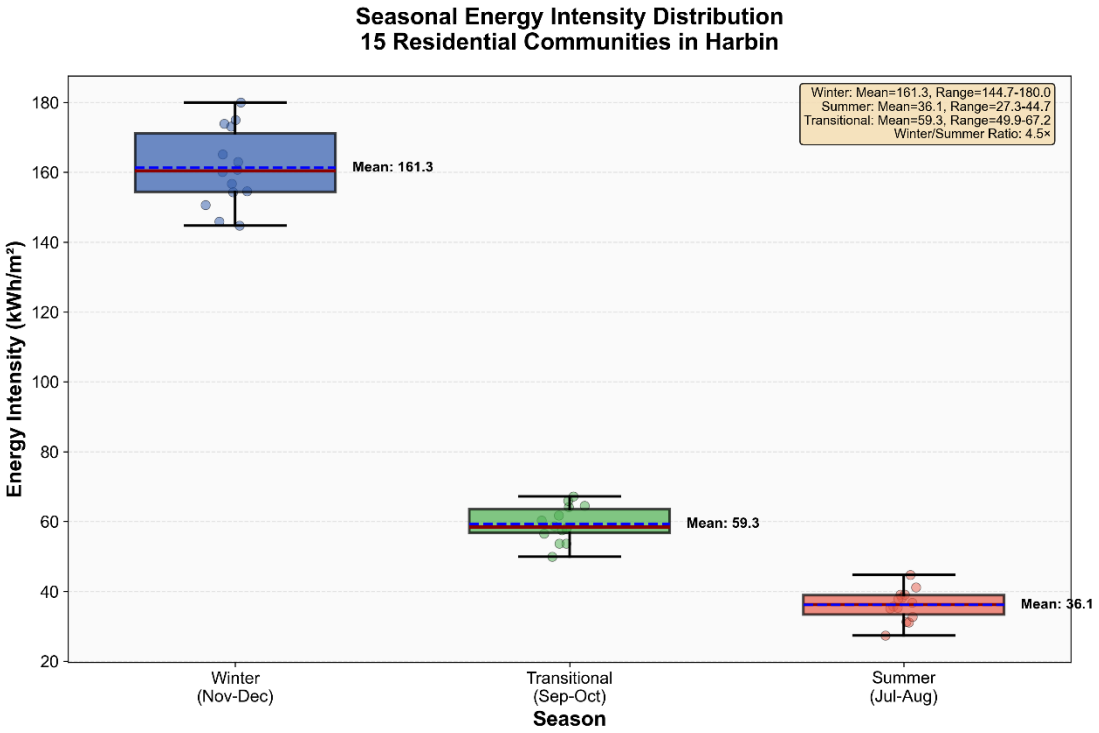

Figure 3. Seasonal energy intensity distribution.

3.2. Correlation analysis between spatial morphology indicators and seasonal energy use

Spearman's correlation analysis reveals a consistent seasonal shift in dominant morphological predictors (Figure 4). In winter and the transitional season, development intensity indicators lead: Building Density (r = 0.649), FAR (r = 0.463), and Building Layout Pattern (r = 0.526) drive winter EUI, while FAR becomes the strongest transitional predictor (r = 0.819). Higher density and FAR increase total heated volume, expand exterior surface exposure, and reduce lower-floor solar access. Summer EUI, by contrast, is governed by three-dimensional configuration: Sky View Factor (r = 0.476), Building Layout Pattern (r = 0.467), and Height Standard Deviation (r = −0.429). Greater height variation creates shading and improves airflow, while open,

uniform layouts amplify solar gain and restrict ventilation. This intensity-driven vs configuration-driven seasonal split defines the SMKF sets used in the regression models below.

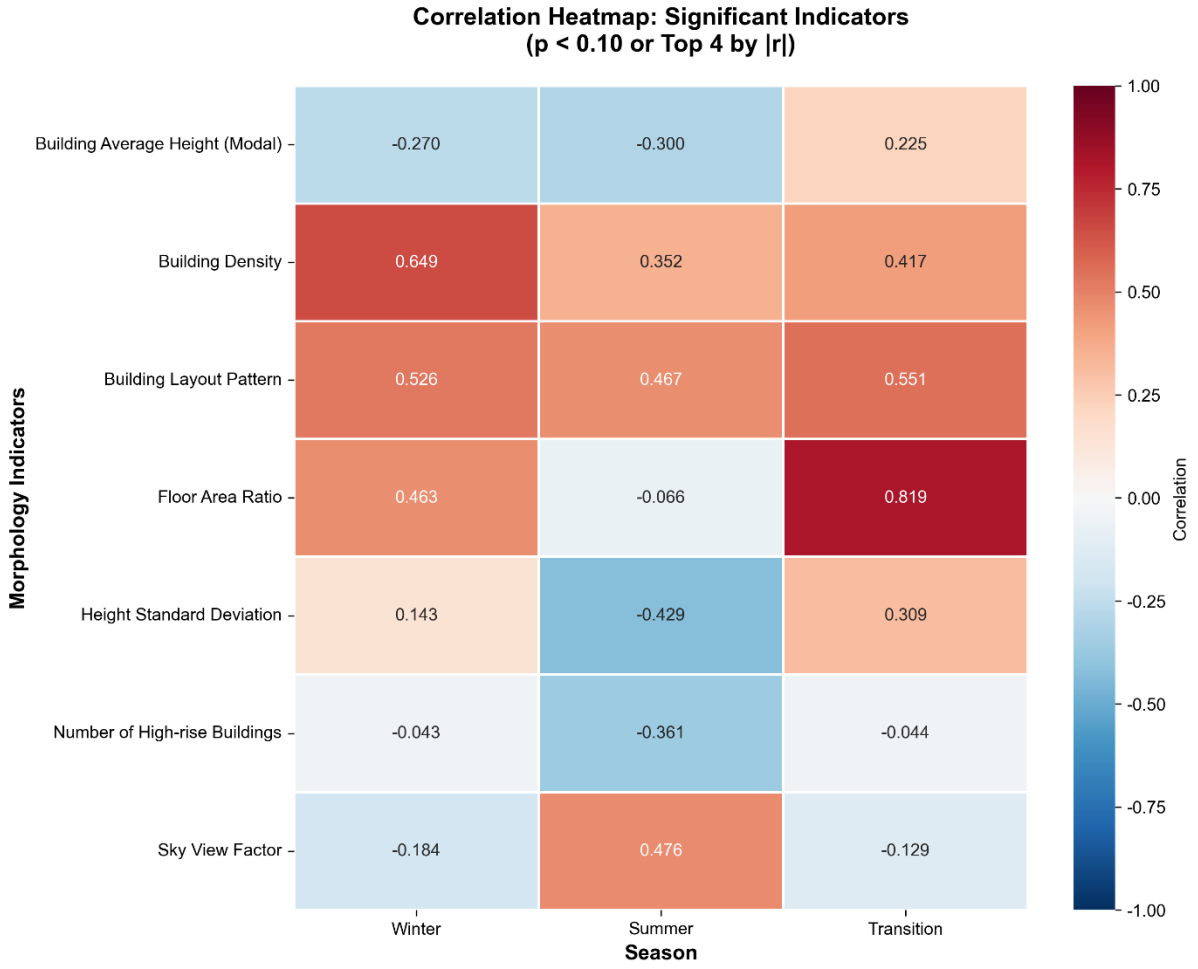

Figure 4. Correlation heatmap of significant indicators.

3.3. Season-specific regression models and morphological drivers of energy use

The three regression models confirm that spatial morphology explains a substantial proportion of seasonal EUI variance (Figure 5). The transitional season model achieved the best fit ($R^2 = 0.725$; adjusted $R^2 = 0.651$),

followed by winter (R^2 = 0.697; adjusted R^2 = 0.647), and summer (R^2 = 0.620; adjusted R^2 = 0.467). All models passed diagnostic tests for normality, independence, and outlier influence.

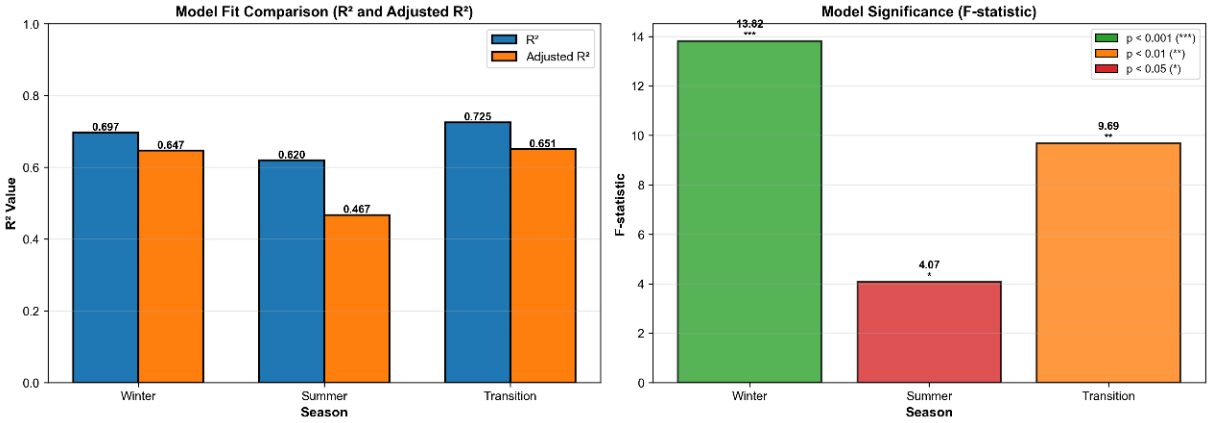

Figure 5. Model performance comparison.

Standardized regression coefficients (Figure 6) further clarify the relative importance of each SMKF. In winter, Building Density (β = 0.682) and FAR (β = 0.576) are the dominant drivers, reflecting how compact, high-density blocks increase heated volume and reduce passive solar gain to lower floors. In summer, the Number of High-rise Buildings (β = 0.842) and Sky View Factor (β = 0.675) dominate, indicating that tall, open configurations amplify solar exposure and restrict ventilation. The transitional season is led by FAR (β = 0.799) and Building Density (β = 0.376), with Height Standard Deviation playing a negligible role (β = 0.035).

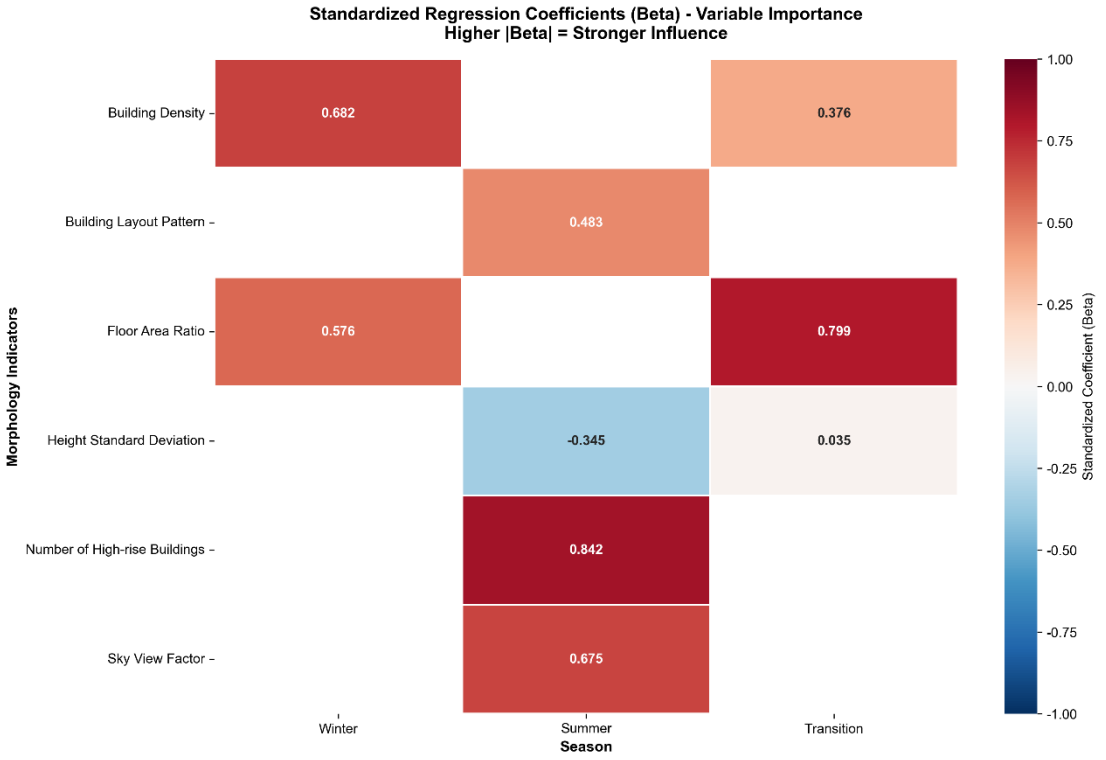

Figure 6. Standardized coefficients heatmap.

These results carry direct implications for climate-resilient neighbourhood planning. First, FAR and building density should be treated as primary energy-performance levers in cold-region development control. Moderate, well-distributed density outperforms both extremes: very low density incurs high heating demand per unit area due to large exposed surface-to-volume ratios, while very high density amplifies total heating loads and degrades daylight access. Planners designing urban renewal frameworks for cold-region cities should specify FAR thresholds informed by seasonal EUI targets rather than by annual averages alone.

Second, building layout pattern matters across all seasons. Articulated, mixed-typology layouts consistently outperform uniform row-block arrangements in energy efficiency. Planning guidelines for new residential areas or redevelopment schemes should discourage monotypic layout configurations and instead promote the mixing of slab-row and point-tower typologies to balance heating efficiency and summer ventilation.

Third, vertical diversity — measured here as Height Standard Deviation — is a key summer cooling strategy. Neighbourhoods with varied building heights create self-shading microenvironments and promote airflow. Planners can encode this principle into height zoning rules that require a mix of low-rise and high-rise buildings within a given residential block, rather than specifying a single maximum height.

Fourth, Sky View Factor should be incorporated as a climate-resilience indicator in spatial performance evaluations. Limiting courtyard openness and avoiding excessively open layouts can reduce summer cooling loads while maintaining adequate daylight. Specific SVF benchmarks could be established for cold-region residential blocks and tested against both summer and winter EUI targets.

Taken together, these morphological levers align with the conference theme of planning pathways to resilience and quality of life. Embedding seasonal energy performance criteria — FAR, building height diversity, layout pattern, and SVF — into neighbourhood planning standards and urban renewal processes would allow cold-region cities to reduce energy vulnerability across all seasons, strengthen climate resilience, and improve residential environmental quality simultaneously.

4. Conclusion

This study examined how spatial morphology shapes seasonal building energy use in 15 residential neighborhoods in Harbin, China, using a combined simulation and statistical modelling approach. Three key findings emerge.

First, winter dominates annual energy demand — at approximately 4.5 times the summer figure — but transitional and summer seasons together account for 37% of total seasonal energy use, confirming that a seasonal perspective is essential for effective energy planning in severely cold regions.

Second, urban form indicators — particularly FAR, building density, and building layout pattern — are significantly and positively associated with EUI across all seasons. The dominant morphological drivers, however, shift with the season: development intensity (FAR and density) governs winter and transitional season consumption, while three-dimensional configuration and openness (height diversity and Sky View Factor) become critical in summer.

Third, the three regression models (adjusted R^2 = 0.467 to 0.651) demonstrate that spatial morphology alone can explain a substantial portion of neighborhood-scale seasonal energy variation, providing a practical basis for morphology-based planning guidance.

For practice, these findings call for the integration of seasonal energy performance metrics into development control and neighborhood renewal frameworks in severely cold cities. Planning tools should enable testing of proposed morphological configurations — FAR, building height distribution, layout typology, and sky view factor — against winter heating, summer cooling, and transitional-season energy benchmarks, rather than relying on annual averages. Mixed-typology layouts, moderate but well-distributed density, and enhanced building height variation are recommended as core morphological strategies for climate-resilient residential planning.

Limitations include the relatively small sample (15 neighborhoods in one city) and the assumption of uniform building envelope performance and occupant behaviour across all sites. These constraints mean that simulated EUI differences reflect morphological effects only, independent of construction quality or lifestyle variation. Future research should expand the sample size and geographic scope, incorporate real-world energy monitoring data to validate simulation outputs, and extend the morphological indicator system to include vegetation, facade materials, and microclimate variables. Multi-objective optimization approaches that simultaneously address energy efficiency, thermal comfort, and urban livability would further strengthen the planning applicability of these findings.

Funding

This research was funded by the Heilongjiang Provincial Natural Science Foundation of China, grant number LH2023E050; Heilongjiang Province Social Science Research Planning Foundation, grant number 22GLC275; Heilongjiang Postdoctoral Found, grant number LBH-Z22158.

5. References

Adilkhanova, I., Santamouris, M., & Yun, G.Y., (2023) 'Coupling urban climate modeling and city-scale building energy simulations with the statistical analysis: Climate and energy implications of high albedo materials in seoul', *Energy and Buildings*, 290, p113092.

Aldawoud, A., & Clark, R., (2008) 'Comparative analysis of energy performance between courtyard and atrium in buildings', *Energy and Buildings*, 40(3), p209–214.

Ali, U., Shamsi, M.H., Hoare, C., Mangina, E., & O'Donnell, J., (2021) 'Review of urban building energy modeling (UBEM) approaches, methods and tools using qualitative and quantitative analysis', *Energy and Buildings*, 246, p111073.

Balali, Y., Chong, A., Busch, A., & O'Keefe, S., (2023) 'Energy modelling and control of building heating and cooling systems with data-driven and hybrid models—a review', *Renewable and Sustainable Energy Reviews*, 183, p113496.

Cai, C. et al., (2025) 'Bi-directional mapping of morphology metrics and 3D city blocks for enhanced characterisation and generation of urban form', *Sustainable Cities and Society*, 129, p106441.

Ferrando, M., Causone, F., Hong, T., & Chen, Y., (2020) 'Urban building energy modeling (UBEM) tools: A state-of-the-art review of bottom-up physics-based approaches', *Sustainable Cities and Society*, 62.

Guillén-Mena, V., Martin-Escudero, K., & Irulegi, O., (2024) 'Integration of building archetypes and typological urban forms to assess energy performance and thermal comfort: Proposal of suitable

parameters for latin America - vanessa guillén-mena, koldobika martin-escudero, olatz irulegi, 2025', *Environment and Planning B: Urban Analytics and City Science*.

Han, D. et al., (2025) 'Cooling effects and energy-saving potential of urban vegetation in cold-climate cities: A comparative study using regression and coupled simulation models', *Urban Climate*, 59, p102268.

Hao, Z., Zhang, X., Xie, J., Yin, K., & Liu, J., (2022) 'Balance point temperature and heating degree-days in different climate conditions for building energy efficiency applications', *Building and Environment*, 216, p109013.

Khalvandi, R., & Karimimoshaver, M., (2023) 'The optimal ratio in the street canyons: Comparison of two methods of satellite images and simulation', *Building and Environment*, 229, p109927.

Leng, H., Chen, X., Ma, Y., Wong, N.H., & Ming, T., (2020) 'Urban morphology and building heating energy consumption: Evidence from harbin, a severe cold region city', *Energy and Buildings*, 224, p110143.

Li, H., Zheng, J., Zhang, Y., & Zhang, R., (2025) 'Urban morphology and residential building net-zero energy performance: A global *meta*-analysis', *Energy and Buildings*, 346, p116142.

Lin, Z. et al., (2024) 'Characterizing the seasonal relationships between urban heat island and surface energy balance fluxes considering the impact of three-dimensional urban morphology', *Building and Environment*, 265, p112017.

Liu, G. et al., (2025) 'Assessing urban morphology effects on residential building electricity consumption via explainable machine learning: Evidence from China's hot summer and warm winter zone', *Energy and Buildings*, 345, p116063.

Liu Y., & Ren G., (2018) 'Analysis of heating intensity in Harbin City based on degree-hour method', *Journal of Natural Resources*, 33(1), p139–148.

Menberg, K., Heo, Y., & Choudhary, R., (2016) 'Sensitivity analysis methods for building energy models: Comparing computational costs and extractable information', *Energy and Buildings*, 133, p433–445.

Pan, W. et al., (2022) 'Morphological Pattern of Building Clusters in Cold Regions: Evidence from Harbin', *International Journal of Environmental Research and Public Health*, 19(24), p17083.

Quan, S.J., & Li, C., (2021) 'Urban form and building energy use: A systematic review of measures, mechanisms, and methodologies', *Renewable and Sustainable Energy Reviews*, 139, p110662.

Quan, S.J., Xue, Y., & Li, C., (2025) 'Nonlinearity in the relationships between urban form and residential energy use intensity', *Applied Energy*, 383(C).

Rahimi Gharibvand, F. et al., (2025) 'Neighborhood-scale energy impacts of renewal initiatives: Evidence from cold-climate cities in iran', *Sustainable Cities and Society*, 132, p106821.

Shen, P., & Wang, H., (2024) 'Archetype building energy modeling approaches and applications: A review', *Renewable and Sustainable Energy Reviews*, 199, p114478.

Shen, X., & Liu, B., (2016) 'Changes in the timing, length and heating degree days of the heating season in central heating zone of China | scientific reports', *Scientific Reports*.

Song, S., Leng, H., Xu, H., Guo, R., & Zhao, Y., (2020) 'Impact of urban morphology and climate on heating energy consumption of buildings in severe cold regions', *International Journal of Environmental Research and Public Health*, 17(22), p8354.

Staffell, I., Pfenninger, S., & Johnson, N., (2023) 'A global model of hourly space heating and cooling demand at multiple spatial scales', *Nature Energy*, 8(12), p1328–1344.

Sun, C., Lian, W., Liu, L., Dong, Q., & Han, Y., (2022) 'The impact of street geometry on outdoor thermal comfort within three different urban forms in severe cold region of China', *Building and Environment*, 222, p109342.

Wang, D., Dong, Q., & Sun, C., (2025) 'Evaluating the adaptation potential and retrofitting effectiveness of existing residential buildings in severe cold regions of China under climate change', *Building and Environment*, 278, p112982.

Wang, M., & Dong, Y., (2025) 'Impact of residential morphology on outdoor thermal comfort and building energy consumption in winter and summer: A case study', *Urban Climate*, 61, p102479.

Wang, Y., Sun, G., Wu, Y., & Rosenberg, M.W., (2024)(a) 'Urban 3D building morphology and energy consumption: Empirical evidence from 53 cities in China', *scientific reports*.

Wang, Y., Sun, G., Wu, Y., & Rosenberg, M.W., (2024)(b) 'Urban 3D building morphology and energy consumption: Empirical evidence from 53 cities in China', *Scientific Reports*, 14(1), p12887.

Wang, Z., & Gadi, M., (2024) 'Optimal HVAC setpoints for energy efficiency and thermal comfort in Chinese residential buildings', *Journal of Building Engineering*, 96, p110286.

Xu, X., Dong, Q., & Zhen, M., (2024) 'Assessing effects of future climate change on outdoor thermal stress and building energy performance in severe cold region of China', *Building and Environment*, 251, p111236.

Yi, D.H., Choi, S., Kim, D.-W., & Yoon, S., (2025) 'Quantifying urban building shading effect for data-driven building energy modeling', *Building and Environment*, p114011.

Zhao, Y. et al., (2024) 'Impact of urban form on building energy consumption in different climate zones of China', *Energy and Buildings*, 320, p114579.

Zhou, Y., Liu, H., Xiong, X., & Li, X., (2024) 'Morphology optimization of residential communities towards maximizing energy self-sufficiency in the hot summer cold winter climate zone of China', *Land*, 13(3), p1–24.